

## Filmwise condensation of a pure fluid and a binary mixture in a bundle of enhanced surface tubes <sup>☆</sup>

M. Belghazi <sup>a</sup>, A. Bontemps <sup>b,\*</sup>, C. Marvillet <sup>a</sup>

<sup>a</sup> *Groupement pour la Recherche sur les Echangeurs Thermiques (GRETh), DRN/DTP, CEA Grenoble, 17, avenue des martyrs, 38 054 Grenoble cedex 9, France*

<sup>b</sup> *Laboratoire des Ecoulements Géophysiques et Industriels (LEGI/GRETh) Université Joseph Fourier, Grenoble, France*

Received 24 October 2001; accepted 8 February 2002

### Abstract

An experimental study has been carried out to investigate the characteristics of condensation in a bundle of horizontal tubes. These tubes have different types of external surfaces: smooth surface (1D), low trapezoidal fins with several fin pitches (2D) and specific fins (3D, C+ tube). The used fluids are either pure refrigerant (HFC 134a) or binary mixture of refrigerants (HFC 134a/HFC23).

For the pure fluid and a single tube, the influence of fin spacing has been studied (11, 19, 26, 32 and 40 fins/inch) and a comparison has been made with the Gewa C+ tube. The results were analysed with the Beatty and Katz theory and compared to a specific model, taking into account both gravity and surface tension effects, developed for the Gewa C+ tube.

For the bundle and for a pure fluid, the inundation of the lowest tubes has a strong effect on the Gewa C+ tubes performances contrary to the finned tubes. For the mixture the heat transfer coefficient decreases dramatically especially for Gewa C+ tube. © 2002 Éditions scientifiques et médicales Elsevier SAS. All rights reserved.

### 1. Introduction

The ozone depletion and the earth global warming problems force the refrigeration industry to reconsider the nature of fluids used in the refrigerating units. New environment friendly refrigerants such as HydroFluoroCarbons are more and more used either as pure fluids or as mixtures. For example, R134a (pure fluid) is regarded as suitable substitute for R12, whilst R407C (zeotropic mixture) is an alternative to R22. This transition brought us to carry out experiments to determine the Heat Transfer Coefficient (HTC) during condensation of R134a and a zeotropic mixture of R23 and R134a, on horizontal tubes with enhanced surfaces. Two types of surfaces have been studied, integral-fin tubes with trapezoidal fins and tubes with notched fins.

Theoretical models to predict the heat transfer coefficient for single low-finned tubes have been well developed since

the 1940s, in particular with the pioneering work of Beatty and Katz [1]. Their model assumed that the condensate is drained only via gravity. They neglected surface tension forces, which have an important role at the fin tip, since they are responsible for the draining of condensate from the tip to the fin flanks, and because the major part of condensation occurs at the fin tip. The surface tension forces also have a non-beneficial effect because of condensate retention at the underside of the tube. Theoretical models combining both gravity and surface tension forces, are used to predict the HTC of a single horizontal tube with sufficient accuracy. Rose [2] proposed a semi-empirical model for a horizontal tube having trapezoidal fins. He defined an enhancement ratio  $\varepsilon_{\Delta T}$ , as the ratio of the heat transfer coefficient for a finned tube to that for a plain tube, based on plain tube area at the fin root diameter for the same  $\Delta T$  ( $\Delta T = T_{\text{sat}} - T_w$ ). To compare his model to experimental results, Rose used various finned tubes with different pitches, heights and diameters as well as various fluids (water, ethylene glycol, methanol, R113, R11, R12, ...).

The foregoing models for a single tube are not directly applicable to tube banks, since the heat transfer in the lower rows is affected by condensate inundation and the HTC is lower for these tubes. In the literature there are

<sup>☆</sup> This article is a follow-up to a communication presented by the authors at the ExHFT-5 (5th World Conference on Experimental Heat Transfer, Fluid Mechanics and Thermodynamics), held in Thessaloniki in September 24–28, 2001.

\* Correspondence and reprints.

E-mail address: bontempsan@chartreuse.cea.fr (A. Bontemps).

## Nomenclature

$A$	heat exchange surface area	$\text{m}^2$
$b$	fin spacing	$\text{m}$
$C_p$	heat capacity	$\text{J}\cdot\text{kg}^{-1}\cdot\text{K}^{-1}$
$D_e$	diameter at the fin tip	$\text{m}$
$D_h$	hydraulic diameter	$\text{m}$
$D_i$	inner diameter	$\text{m}$
$D_r$	diameter at the fin root	$\text{m}$
$f$	friction factor	
$F$	force	$\text{N}$
$g$	gravity	$\text{m}\cdot\text{s}^{-2}$
$h$	fin height	$\text{m}$
$K$	notches number on each fin flanks	
$L$	plate length	$\text{m}$
$m$	mass flow rate	$\text{kg}\cdot\text{s}^{-1}$
$p$	fin pitch	$\text{m}$
$P$	pressure	$\text{Pa}$
$r$	curvature radius	$\text{m}$
$s$	curvilinear coordinate	$\text{m}$
$t$	fin thickness	$\text{m}$
$U$	overall HTC	$\text{W}\cdot\text{m}^{-2}\cdot\text{K}^{-1}$
$w$	notch width	$\text{m}$
$z$	space between notches	$\text{m}$

### Greek symbols

$\alpha_e$	vapour side HTC	$\text{W}\cdot\text{m}^{-2}\cdot\text{K}^{-1}$
$\alpha_i$	inner HTC	$\text{W}\cdot\text{m}^{-2}\cdot\text{K}^{-1}$

$\alpha_p$	predicted HTC	$\text{W}\cdot\text{m}^{-2}\cdot\text{K}^{-1}$
$\Delta T$	$(T_{\text{sat}} - T_w)$ or $(T_{v,j} - T_w)$	$\text{K}$
$\Delta h_v$	latent heat	$\text{J}\cdot\text{kg}^{-1}$
$\Phi$	retention angle	$\text{rad}$
$\Gamma$	condensate mass flow rate	$\text{W}\cdot\text{m}^{-1}\cdot\text{K}^{-1}$
$\mu$	dynamic viscosity	$\text{Pa}\cdot\text{s}$
$\nu$	kinematic viscosity	$\text{m}^2\cdot\text{s}^{-1}$
$\rho$	density	$\text{kg}\cdot\text{m}^{-3}$
$\sigma$	surface tension	$\text{N}\cdot\text{m}^{-1}$

### Indices

I, II, III, IV	region's index
c	coolant
e	external
f	film condensate
in	water inlet
$j$	row index
$\ell$	liquid
out	water outlet
v	vapour
w	wall

### Dimensionless numbers

$Nu$	Nusselt number
$Pr$	Prandtl number
$Re$	Reynolds number

several approaches to this problem. The simplest consists of multiplication of the heat transfer for a single tube by a factor less than unity, taking into account the row position in the bundle.

There are few experiments on condensation of HFC134a on low finned tubes. In the work of Blanc et al. [3] the HTC on trapezoidal fin tubes (K26) is compared with another type of finned tube together with current theories. Honda et al. [4] measured the row-by-row heat transfer coefficients of HFC134a condensing on a bundle of tubes having 26 fins/inch and a diameter at the fin root of 15.8 mm. Their results are slightly lower than those of Blanc et al. Cheng and Wang [5] and Agrawal et al. [6] conducted experiments on condensation of HFC134a using several types of low finned tubes. The former found that for a vertical column of three tubes with trapezoidal fins no significant inundation effect is observed. The latter have studied the variation of the HTC in function of  $\Delta T$  for a single tube.

Studies covering the condensation of zeotropic mixtures are essentially confined to flat plates and smooth tubes. Hijikata and Himemo [7] conducted experiments using horizontal finned tubes during condensation of the binary mixture (90% R113 + 10% R114), and they found that the tube with high fins (3 mm) is better than the one with small fins (0.8 mm). Honda et al. [8] conducted experiments during

condensation of a downward-flowing zeotropic mixture HFC123/HFC134a (about 9% HFC134a at the test section inlet), on a  $13 \times 15$  (columns  $\times$  rows) staggered bundle of horizontal low finned tubes. Their experimental data show that both the heat and the mass transfer coefficients increased with the row number up to the third (or the second) row, then decreased monotonically with increasing row number, finally to increase at the last row.

## 2. Experimental apparatus and reduction of data

The experimental apparatus consists of a thermosiphon refrigerant loop and a forced circulation coolant (water) loop (Fig. 1). The test rig used in this investigation is basically the same as that used in a previous study [9].

The fluids are either a pure fluid (HFC 134a) or a mixture (HFC 23/HFC 134a). The mixture concentrations indicated in the figures refer to the composition of the refrigerant charged into the boiler.

In the refrigerant loop the vapour is generated in a boiler heated with hot water which is itself heated with an electric heater. The vapour flows toward the test section, passes vertically downwards and condenses outside the water cooled tubes. The test section (Fig. 2) is a stainless

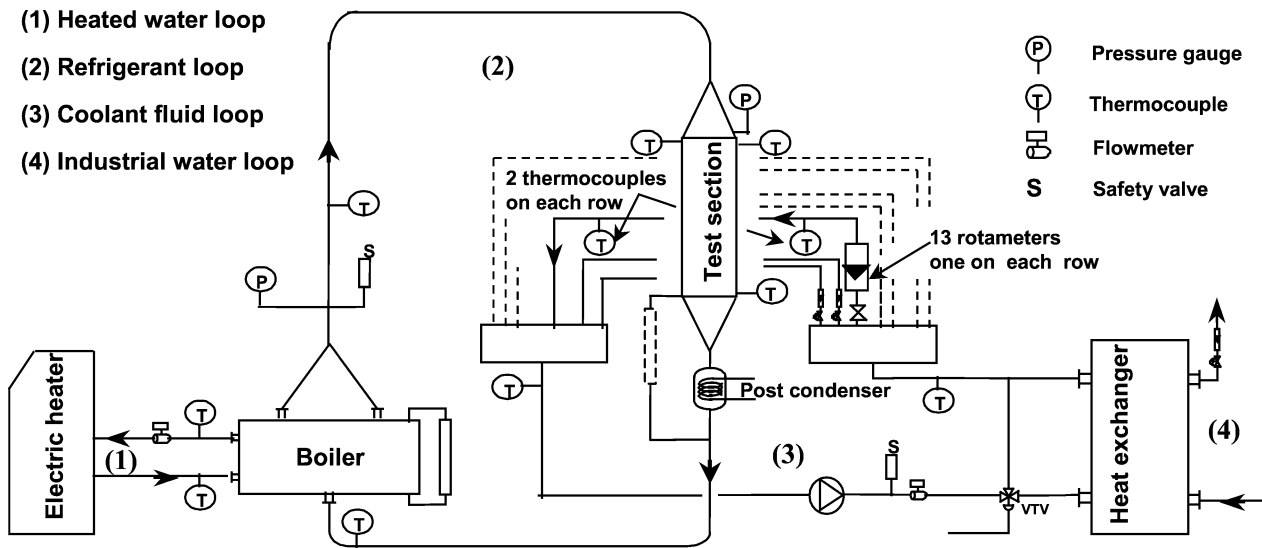


Fig. 1. Test rig.

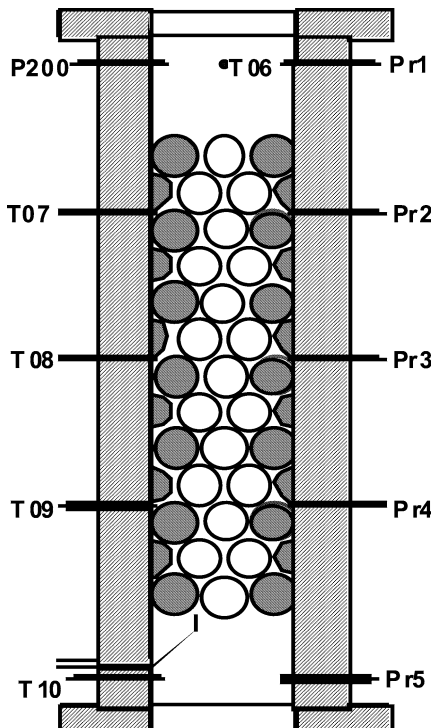


Fig. 2. Test section.

steel duct and contains a staggered copper tube bank consisting of 13 rows, each of 2 (even rows) or 3 tubes (odd rows). The cross-hatched tubes are dummies (no heat exchange), while the others are active. Half tubes are attached to vertical walls of the test section in order to eliminate vapour by-pass. A metallic rod with a diameter of 11 mm was inserted in each active tube in order to increase the water velocity. In this way the heat transfer is enhanced on the coolant side. The horizontal tube pitch is 24 mm, whereas the vertical pitch is 20 mm. The length of the tubes

Table 1  
Tube dimensions (mm)

Tube	$D_r$	$D_e$	$D_i$	$p$	$h$	$t$
Smooth	16.8	16.8	14.2	–	–	–
K11	16	18.9	14	2.31	1.45	0.38
K19	16	18.9	14	1.34	1.45	0.33
K26	15.8	18.8	14	0.97	1.5	0.25
K32	16.2	18.8	14	0.82	1.3	0.2
K40	16.3	18.9	14.4	0.635	1.3	0.16
Gewa C+	17	18.9	14	~0.7	0.96	~0.12

is 300 mm. The characteristics of the tested tubes are given in Table 1.

The vapour temperature inlet was maintained at 40 °C and the vapour velocity is less than 2 m·s<sup>-1</sup>. The vapour temperature is measured by five thermocouples (T06, T07, T08, T09 and T10) in the test section. These thermocouples indicate the same temperatures ( $T_{sat}$ ) during the condensation of HFC134a, in contrast to the condensation of HFC23/HFC134a, where the vapour temperature decreases from the inlet to the outlet of the test section. The temperatures indicated by the five thermocouples are interpolated in order to obtain the vapour temperature in the neighbourhood of each row.

In this study, commercially tubes (Wieland-Werke AG) are used, having a wall thickness of about 1 mm. An indirect Wilson plot method which measures the vapour-side heat transfer coefficient without measuring the wall temperature is employed.

From the measured water temperatures at the inlet and the outlet of each tube and from the measured vapour temperature in the neighbourhood of each row, the overall HTC is calculated as follows:

$$U = \frac{\dot{m}_c C_{p,c}}{\pi D_r} \ln \left( \frac{T_{v,j} - T_{c,j,in}}{T_{v,j} - T_{c,j,out}} \right) \quad (1)$$

where  $j$  refers to the row number.

Table 2  
B values

Tube	Gewa C+	K40	K32	K26	K19	K11
B	1.07	1.19	0.99	0.98	1.08	0.92

The vapour-side HTC  $\alpha_e$  is calculated by the following relation:

$$\frac{1}{\alpha_e} = \frac{1}{U} - \frac{1}{\alpha_i} \frac{D_r}{D_i} - \frac{D_r}{2\lambda_w} \ln\left(\frac{D_r}{D_i}\right) \quad (2)$$

$\alpha_i$  is the inner heat transfer coefficient determined with the Gnielinski correlation [10]:

$$Nu_G = \frac{(f/2)(Re_c - 1000)Pr_c}{1 + 12.7(f/2)^{0.5}(Pr_c^{2/3} - 1)} \quad (3)$$

where  $f$  is the friction factor determined from the following expression:

$$f = (1.58 \ln(Re_c) - 3.28)^{-2} \quad (4)$$

The Gnielinski correlation has been chosen because it has a wide range of applicability,  $2300 < Re < 5 \times 10^6$  and  $0.5 < Pr < 2000$ , thus, it covers both the transition and the turbulent flow regimes. The inner HTC  $\alpha_i$  is expressed as:

$$\alpha_i = B \cdot Nu_G \cdot \frac{\lambda_c}{D_h} \quad (5)$$

where the coefficient  $B$  is determined by the Wilson plot procedure [11]. Table 2 gives the  $B$  values for all tubes tested.

The overall HTC  $U$  has a relative uncertainty of 15%, and the calibration of the inner HTC of K11, K19, K26, K32, K40 and Gewa C+ tubes leads respectively to relative uncertainties of 9.8%, 8.3%, 4.2%, 13% and 3%, 5%, determined using Moffat's method of sequential disturbances. The relative uncertainty of the vapour-side HTC is the quadratic mean of the inner and the overall HTCs, and is equal to 17.9%, 17.1%, 15.6%, 19.8%, 15.2%, 15.8% for the K11, K19, K26, K32, K40 and Gewa C+ tubes respectively.

### 3. Experimental results

#### 3.1. Pure fluid (HFC 134a)

##### 3.1.1. Single tube

Fig. 3 shows the evolution of the HTC of the first row with  $\Delta T$ , during condensation of pure HFC134a on tubes tested in this investigation and on smooth tube tested in a previous work [9]. It can be seen that K32 have the best performances compared to the other trapezoidal fin tubes. A fin spacing of about 0.6 mm is then an optimum to have the best heat transfer coefficient during condensation of HFC134a. Gewa C+, a notched fin tube which have almost the same fin pitch than K40, presents a HTC better than the K32 tube, because notches located at the middle of the fin height, enhance surface tension effects at the fin tip. Then,

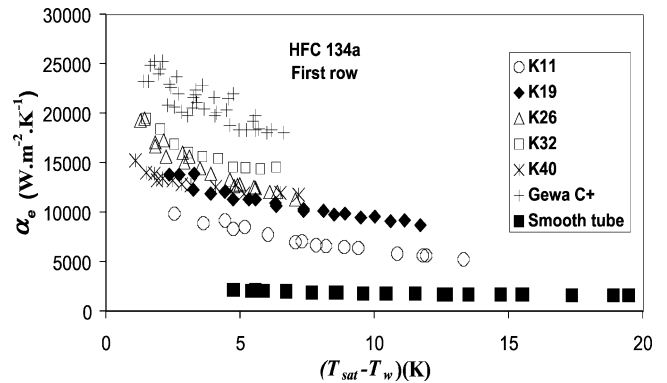


Fig. 3. HTC of the first row during condensation of HFC134a.

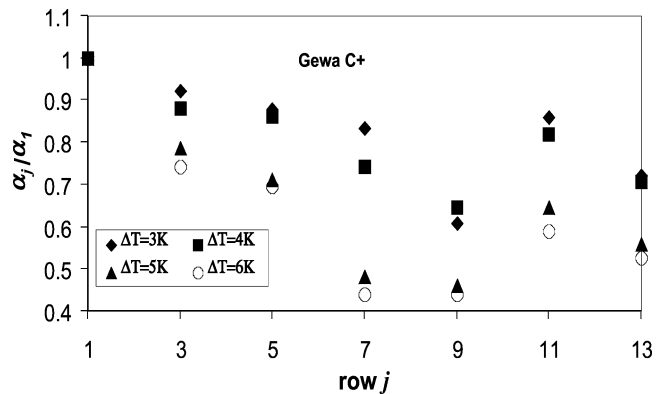


Fig. 4. Evolution of the Gewa C+ HTC along the bundle during condensation of HFC 134a.

the film condensate is thinner and heat transfer performances are better.

To predict the Gewa C+ HTC a theoretical model has been developed. During condensation of pure fluids. It is based on the Nusselt approach but taking the surface tension into account.

##### 3.1.2. Tube bundle

Fig. 4 shows the evolution of the heat transfer coefficient along the bundle. It can be seen that the inundation effect (impinging of deep rows by condensate flowing from upper rows) is important for Gewa C+ tubes in contrast to trapezoidal fin tubes [12] where the deterioration of the HTC is not important. It is noticed also that the more important the Gewa C+ HTC deterioration, the more important  $\Delta T$ .

#### 3.2. Mixture

##### 3.2.1. Single tube

Fig. 5 shows the evolution of the HTC during condensation of two compositions (3% and 6% HFC23) of the binary mixture HFC23/HFC134a on K19 and Gewa C+ tubes. We note a deterioration of the mixture HTC because of the mass transfer induced by the more volatile component (HFC23), which accumulates in the liquid–vapour interface and constitutes a diffusion layer which acts as a thermal resistance.

Contrary to the case of the pure fluid it can be seen from Fig. 5 that the Gewa C+ has the same HTC as the one of the K19 tube. Indeed, as Gewa C+ tube has low fins compared to the other fin tubes, its fins are flooded by the diffusion layer (Fig. 6), and its performances are deteriorated. For the composition (6% HFC 23) and for low  $\Delta T$ 's, where the diffusion layer controls the heat transfer, the K19 and Gewa C+ HTC values tend to the smooth tube HTC values, because the diffusion layer is very thick and screens the fins, then the finned tube is seen as a smooth tube.

3.2.2. Tube bundle

During condensation of mixture outside Gewa C+ bundle the HTC may increase or decrease from the top to the bottom of the tube bank (Fig. 7), depending on the heat flux. Such effect has already been observed by Signe [12] who noted that the HTC on a bundle of smooth tubes increases throughout the bundle. This effect was explained by the fact that the condensate formed on upper rows disturb the diffusion layer, which gives an amelioration of the heat transfer.

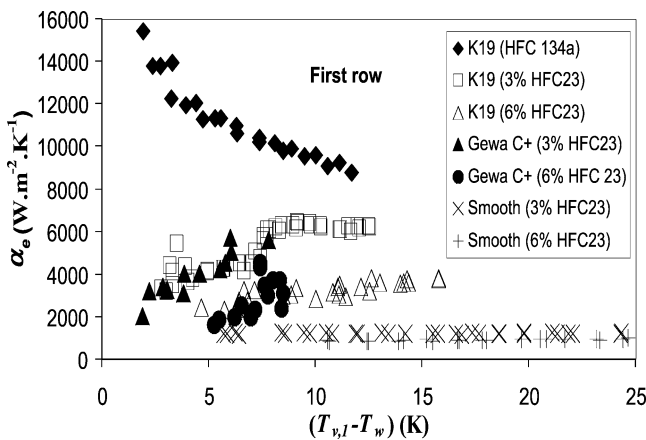


Fig. 5. Evolution of mixture's HTC on Gewa C+ and K19 tubes.

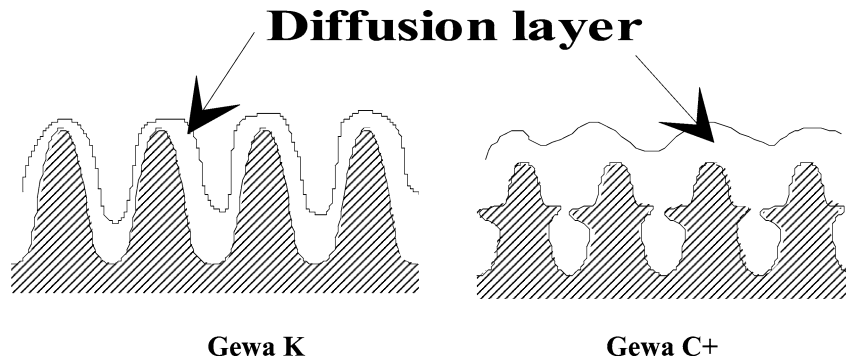


Fig. 6. Flooding of fins by the diffusion layer.

4. Theoretical model

As shown in Fig. 8, the Beatty and Katz model underestimates the HTC of the Gewa C+ tube, because it neglects surface tension effects, which are enhanced by notches located at the fin flanks (Fig. 10). To develop a model predicting the HTC on the Gewa C+ tube, the tube circumference have been divided into a flooded part and an unflooded part.

The flooded part located at the bottom of the tube is referred as an area submerged completely by the condensate because of the capillary retention. We assume that there is no heat transfer in this part of the tube. The retention angle  $\Phi$  (Fig. 9) is calculated by the Rudy and Webb equation [13]:

$$\Phi = \cos^{-1} \left( \frac{4\sigma \cos \theta}{\rho g b D_e} - 1 \right) \tag{6}$$

the unflooded region has been divided into four regions:

- Region I: referred as the upper part of the fin, located above notches;
- Region II: fin area beneath notches;
- Region III: fin area located between notches;
- Region IV: the interfin channel.

It was assumed that the condensate is drained by surface tension in regions I and III, and by gravity in regions II and IV.

The model is based on the Nusselt expressions for condensation on a vertical plate (Eq. (7)), and on horizontal smooth tube (Eq. (8))

$$\alpha_{plate} = 0.943 \left( \frac{\lambda_\ell^3 \rho_\ell (\rho_\ell - \rho_v) g \Delta h_v}{\mu_\ell (T_{sat} - T_w) L} \right)^{1/4} \tag{7}$$

$$\alpha_{tube} = 0.728 \left( \frac{\lambda_\ell^3 \rho_\ell (\rho_\ell - \rho_v) g \Delta h_v}{\mu_\ell (T_{sat} - T_w) D} \right)^{1/4} \tag{8}$$

where  $L$  and  $D$  are plate length and tube diameter, respectively.

Indeed, for regions I and III where only surface tension forces drain condensate, we modify Nusselt's expression (Eq. (7)) by replacing  $\rho_\ell g$  which is a gravity volume force, by an equivalent in terms of surface tension.

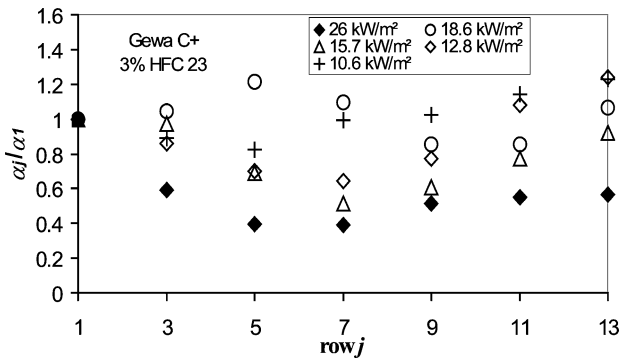


Fig. 7. Evolution of the ratio  $\alpha_j/\alpha_1$  in function of the row number.

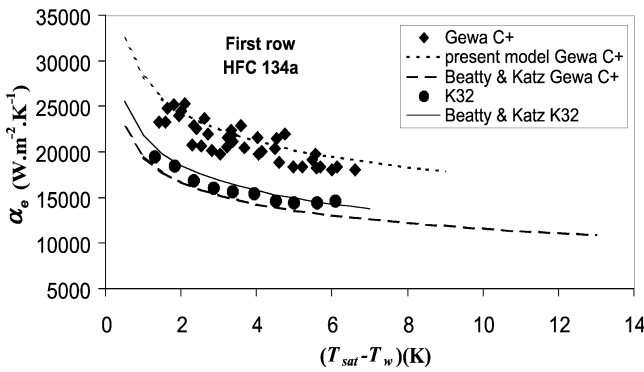


Fig. 8. Experimental and predicted HTC during condensation of HFC 134a on Gewa C+ and K32.

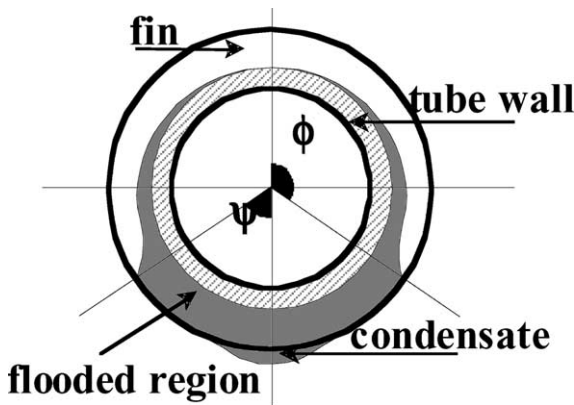


Fig. 9. Retention angle.

Generally the condensation of a fluid having a liquid-vapour interface radius, varying along the wall, induces a pressure variation along the liquid–vapour interface following the equation [14]:

$$\frac{dP}{ds} = \frac{d(\sigma/r)}{ds} \tag{9}$$

Eq. (9) has been expressed in term of a volume force and gives:

$$dF_\sigma = \sigma \frac{d(1/r)}{ds} dV \tag{10}$$

where  $dV$  is a condensate volume control.

For a condensate film surface having two different radius  $r_t$  and  $r_b$  as shown in Fig. 11, the curvature derivative can be written as:

$$\frac{d(1/r)}{ds} \approx \frac{1}{h} \left( \frac{1}{r_b} - \frac{1}{r_t} \right) \tag{11}$$

where  $h$  is the fin height.

Combining Eqs. (10) and (11) we have:

$$\frac{dF_\sigma}{dV} \approx \frac{\sigma}{h} \left( \frac{1}{r_b} - \frac{1}{r_t} \right) \tag{12}$$

The Gewa C+ HTC, calculated with reference to the surface of tube having  $D_r$  as a diameter, is a function of the HTC's of regions I, II, III and IV and is given by:

$$\alpha_p A_r = \eta(\alpha_I A_I + \alpha_{II} A_{II} + \alpha_{III} A_{III}) + \alpha_{IV} A_{IV} \tag{13}$$

where  $\eta$  is the fin efficiency,

$$A_I = 2 \frac{\Phi}{\pi} K w e_1 / p \tag{14}$$

$$A_{II} = 2 \frac{\Phi}{\pi} K w e_2 / p \tag{15}$$

$$A_{III} = 2 \frac{\Phi}{\pi} K z h / p = 2 \frac{\Phi}{\pi} K z (e_1 + e_2 + e_3) / p \tag{16}$$

$$A_{IV} = \frac{\Phi}{\pi} K \pi D_r b / p \tag{17}$$

$$A_r = \pi D_r,$$

where  $K$  is the notch number on one side of a fin flank and  $p$  is the fin pitch. Assuming that (Fig. 10):

$$r_t = t/2, \quad r_{b1} = b/4, \quad r_{b2} = b/2$$

The acting force in the region I is given by:

$$\left. \frac{dF_\sigma}{dV} \right|_{\text{Region I}} = \frac{\sigma}{e_1} \left( \frac{1}{r_t} + \frac{1}{r_{b1}} \right) = \frac{\sigma}{e_1} \left( \frac{2}{t} + \frac{4}{b} \right) \tag{18}$$

substituting  $\rho g$  in Eq. (7) by Eq. (18) leads to:

$$\alpha_I = 0.943 \left( \frac{\lambda_\ell^3 (\rho_\ell - \rho_v) \Delta h_v}{\mu_\ell (T_{sat} - T_w) e_1} \right)^{1/4} \left( \frac{\sigma}{e_1} \left( \frac{2}{t} + \frac{4}{b} \right) \right)^{1/4} \tag{19}$$

In the same manner in region III:

$$\left. \frac{dF_\sigma}{dV} \right|_{\text{Region III}} = \frac{\sigma}{h} \left( \frac{1}{r_t} + \frac{1}{r_{b2}} \right) = \frac{2\sigma}{h} \left( \frac{1}{t} + \frac{1}{b} \right) \tag{20}$$

$$\alpha_{III} = 0.943 \left( \frac{\lambda_\ell^3 (\rho_\ell - \rho_v) \Delta h_v}{\mu_\ell (T_{sat} - T_w) h} \right)^{1/4} \left( \frac{2\sigma}{h} \left( \frac{1}{t} + \frac{1}{b} \right) \right)^{1/4} \tag{21}$$

In region II, the condensate is drained by gravity and the HTC is given by:

$$\alpha_{II} = 0.943 \left( \frac{\lambda_\ell^3 \rho_\ell (\rho_\ell - \rho_v) g \Delta h_v}{\mu_\ell (T_{sat} - T_w) e_2} \right)^{1/4} \tag{22}$$

The HTC in the interfin channel is given using Eq. (8) as follows:

$$\alpha_{\text{channel}} = 0.728 \left( \frac{\lambda_\ell^3 \rho_\ell (\rho_\ell - \rho_v) g \Delta h_v}{\mu_\ell (T_{sat} - T_w) D_r} \right)^{1/4} \tag{23}$$

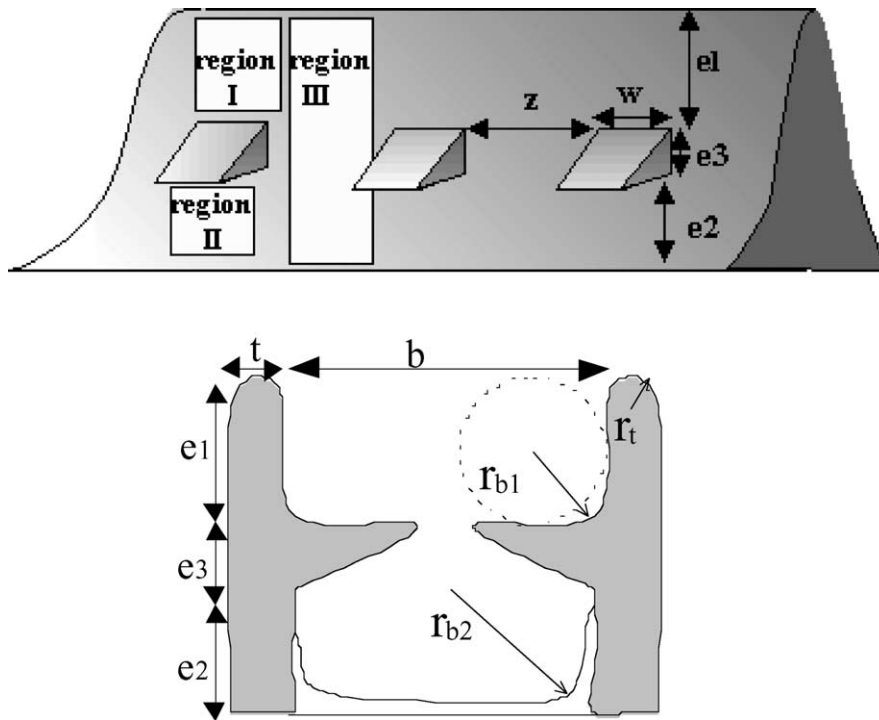


Fig. 10. The shape of Gewa C+ tube.

The condensate formed on fins is collected by the interfin channel, so the actual HTC corresponding to the region IV is smaller than the one calculated by Eq. (23) because the film condensate is thicker. To take this phenomenon into account we use another expression of the Nusselt formula (Eq. (24)):

$$\alpha_{IV} = 1.51 Re_f^{-1/3} \left( \frac{v_\ell^2}{\lambda_\ell^3 g} \right)^{-1/3} \quad (24)$$

where

$$Re_f = 4 \frac{\Gamma}{\mu_\ell} \quad \text{and} \quad \Gamma = \Gamma_{\text{channel}} + \Gamma_{\text{fin}}$$

$$\Gamma_{\text{channel}} = \frac{\alpha_{\text{channel}}(T_{\text{sat}} - T_w) A_{IV}}{\Delta h_v} \quad (25)$$

$$\Gamma_{\text{fin}} = \eta \frac{(\alpha_I A_I + \alpha_{II} A_{II} + \alpha_{III} A_{III})(T_{\text{sat}} - T_w)}{\Delta h_v} \quad (26)$$

Fig. 8 shows that the present model predicts very accurately the Gewa C+ HTC, without fitting any parameter. The deviation from experimental results is less than 10%.

### 5. Conclusion

The present investigation brings us to draw the following concluding remarks:

Experimental data for condensation of HFC134a on five commercially available, copper, integral fin tubes, show an optimum fin spacing of about 0.6 mm.

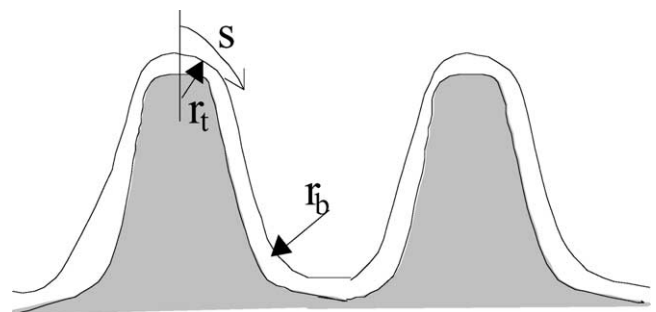


Fig. 11. Variation of the vapour interface radius.

The Gewa C+ tube (notched tube) has been tested and gives an enhancement of about 30% of the best integral fin tubes (K32). Notches drawn on fin flanks enhance the surface tension effect. The inundation effect during condensation of HFC134a is important for high  $\Delta T$ .

For the mixtures, experimental results show that, due to the zeotropic character of the mixture tested (HFC23/HFC134a), the HTC is deteriorated dramatically. Contrary to the pure fluid case, the Gewa C+ tube gives no enhancement compared to the K19 tube.

The model developed for a single Gewa C+ tube, takes into account surface tension effects, and predicts accurately the present experimental data.

Work is currently in progress to develop a model, based on the condensation curve method, predicting heat transfer during condensation of binary mixtures outside a bundle of Gewa C+.

## References

- [1] K.O. Beatty, D.L. Katz, Condensation of vapors on outside of finned tubes, *Chemical Engrg. Progress* 44 (1948) 55–77.
- [2] J.W. Rose, An approximation equation for the vapour-side heat-transfer coefficient for condensation on low-finned tubes, *Internat. J. Heat Mass Transfer* 37 (1994) 865–875.
- [3] P. Blanc, A. Bontemps, C. Marvillet, Condensation heat transfer of HCFC22 and HFC134a outside a bundle of horizontal low finned tubes, in: *Proc. Symp. CFC's, The Day After, Padova, Italy, 1994*, pp. 635–642.
- [4] H. Honda, H. Takamatsu, N. Takada, T. Yamasaki, Condensation of HFC 134a and HFC 123 in a staggered bundle of horizontal finned tubes, in: *Proc. Eurotherm n°47, Heat Transfer in Condensation, Paris, 1995*, pp. 110–115.
- [5] W.Y. Cheng, C. Wang, Condensation of R-134a on enhanced tubes, *ASHRAE Trans.* 10 (1) (1994) 809–817.
- [6] K.N. Agrawal, B. Moharty, R. Kumar, H.K. Varma, Enhancement of heat transfer rates during condensation of refrigerants over horizontal finned tubes, in: *Proc. Symp. Two Phase Flow Modelling and Experimentation, Vol. 1, 1999*, pp. 505–510.
- [7] K. Hijikata, N. Himemo, Condensation of azeotropic and nonazeotropic binary vapor mixtures, *Ann. Rev. Heat Transfer* 3 (2) (1990) 39–83.
- [8] H. Honda, M. Takuma, N. Takada, Condensation of downward-flowing zeotropic mixture HFC-123/HFC-134a on a staggered bundle of horizontal low-finned tubes, *J. Heat Transfer* 121 (1999) 405–412.
- [9] M. Belghazi, A. Bontemps, J. Signe, C. Marvillet, Condensation heat transfer of a pure fluid and binary mixture outside a bundle of smooth horizontal tubes, Comparison of experimental results and a classical model, *Internat. J. Refrigeration* 24 (2001) 841–855.
- [10] V. Gnielinski, New equation for heat and mass transfer in turbulent pipe and channel flow, *Internat. Chem. Engrg.* 16 (2) (1976) 359–368.
- [11] E.E. Wilson, A basis for rational design of heat transfer apparatus, *Trans. ASME* 37 (1915) 47–70.
- [12] J.C. Signe, Condensation de mélanges non azéotropes de fluides frigorigènes à l'extérieur d'un faisceau de tubes horizontaux, Ph.D. Thesis, Université Joseph Fourier, Grenoble, France, 1999.
- [13] T.M. Rudy, R.L. Webb, An analytical model to predict condensate retention on horizontal integral-fin tubes, *ASME J. Heat Transfer* 107 (1985) 361–368.
- [14] R. Gregorig, Film condensation on finely rippled surfaces with consideration of surface tension, *Z. Angew. Math. Phys.* 5 (1954) 36–49.